Supporting Information

Dissolvable Microneedles Coupled with Nanofiber Dressings Eradicate Biofilms *via* Effectively Delivering a Database Designed Antimicrobial Peptide

Yajuan Su[†], Valerio Luca Mainardi[#], Hongjun Wang[†], Alec McCarthy[†], Yu Shrike Zhang[#], Shixuan Chen[†], Johnson V. John[†], Shannon L. Wong[‡], Ronald R. Hollins[‡], Guangshun Wang[ζ,*], and Jingwei Xie[†,*]

[†]*Department of Surgery-Transplant and Mary & Dick Holland Regenerative Medicine Program, University of Nebraska Medical Center, Omaha, Nebraska 68130, United States*

[#]*Division of Engineering in Medicine, Department of Medicine, Brigham and Women's Hospital, Harvard Medical School, Cambridge, MA 02139, United States*

[‡]*Department of Surgery-Plastic Surgery, University of Nebraska Medical Center, Omaha, Nebraska 68130, United States*

[ζ]*Department of Pathology and Microbiology, College of Medicine, University of Nebraska Medical Center, University of Nebraska Medical Center, Omaha, Nebraska 68198, United States*

To whom the correspondence should be addressed.

[*]E-mail: jingwei.xie@unmc.edu (J. Xie) and gwang@unmc.edu (G. Wang)

Phone: +1 (402) 5599442

Fax: +1(402) 5597521

METHODS

Microneedle Dissolution. The microneedle dissolution was evaluated in the biofilm created on human skin wounds *ex vivo*. A Janus-type dressing was first inserted into the biofilm by applying manual pressure. The dressing was removed each 1 min for observation and evaluation till the microneedle arrays were completely dissolved.

FITC-dextran Distribution in Biofilm after Administration of FITC-dextran-incorporated Microneedle Arrays. The FITC-dextran (Mw=4,000, Sigma-Aldrich, St. Louis, MO, USA) with the same concentration and similar molecular weight as W379 peptides was first incorporated to the PVP microneedle array. The FITC-dextran distribution was viewed *in situ* after administration of the microneedle array to the biofilm created on human skin wounds *ex vivo* using a Zeiss 880 laser scanning confocal microscope (CLSM) under the multi slice mode.

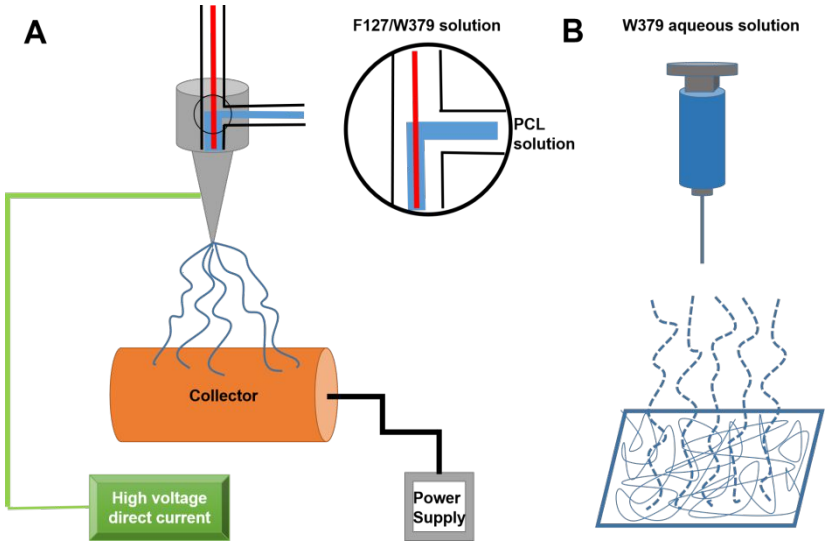

Figure S1. (A) Schematic illustrating co-axial electrospinning and preparation of pluronic F127/W379-PCL nanofiber dressings. (B) Schematic illustrating electrospray deposition of engineered peptide W379 to pluronic F127/W379-PCL nanofiber membranes to form pluronic F127/W379-PCL-S nanofiber dressings.

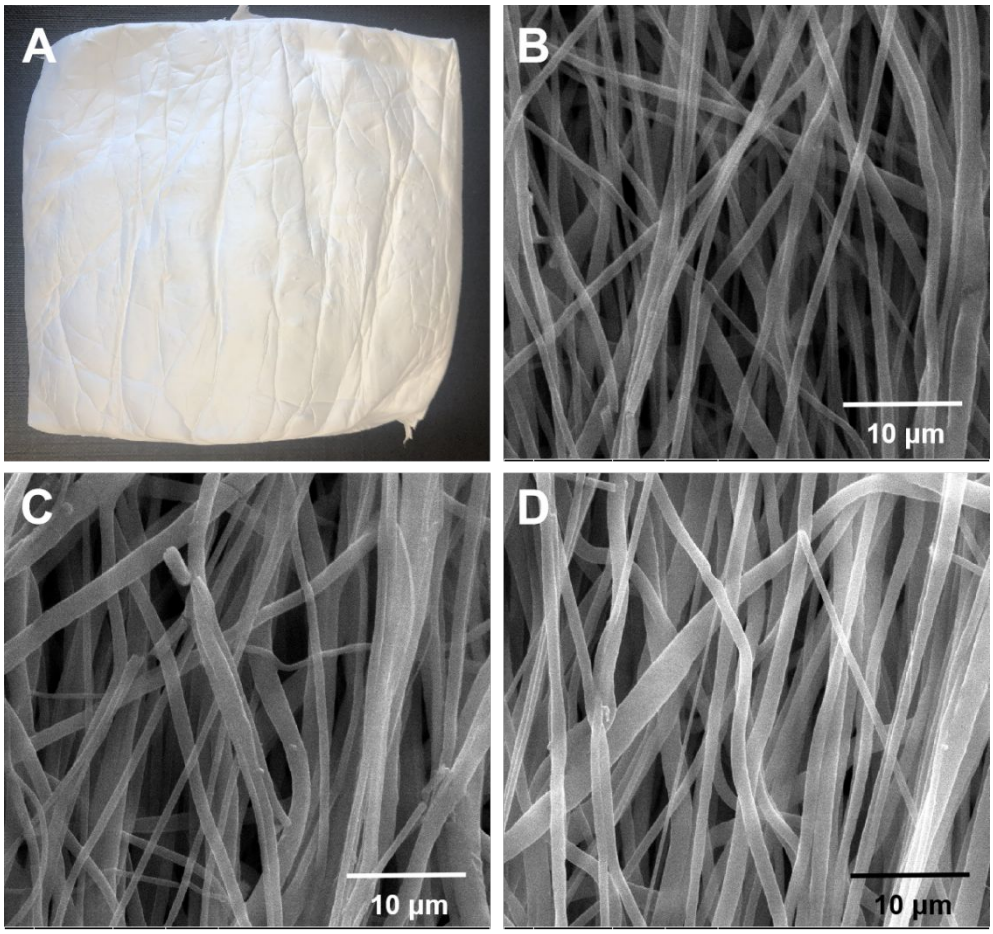

Figure S2. Morphology of nanofiber dressings. (A) Photograph of pluronic F127/W379-PCL core-shell nanofiber membranes. (B−D) SEM images of pluronic F127-PCL core-shell nanofibers, pluronic F127/W379-PCL core-shell nanofibers, and pluronic F127/W379-PCL-S nanofibers.

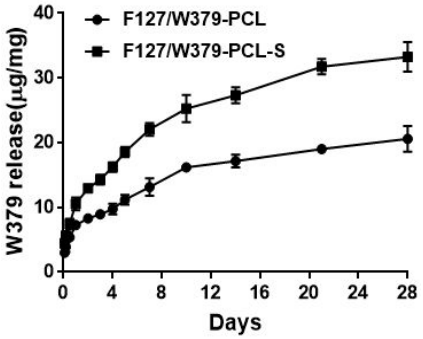

Figure S3. *In vitro* release profiles of the W379 peptide from F127/W379-PCL core−shell nanofibers and after electrospray deposition of W379 (F127/W379-PCL-S).

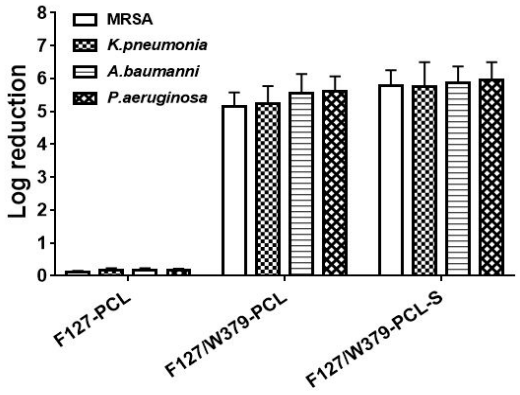

Figure S4. *In vitro* antibacterial efficacy test of F127/W379-PCL core−shell nanofibers. The bacterial solution was diluted into 1.0×10^7 CFU/mL in PBS. One milligram of PCL or F127/W379- PCL core−shell nanofiber membranes was co-incubated with the bacterial solution for 2 h at 37 °C. Total remaining bacteria were determined by culturing on agar plates.

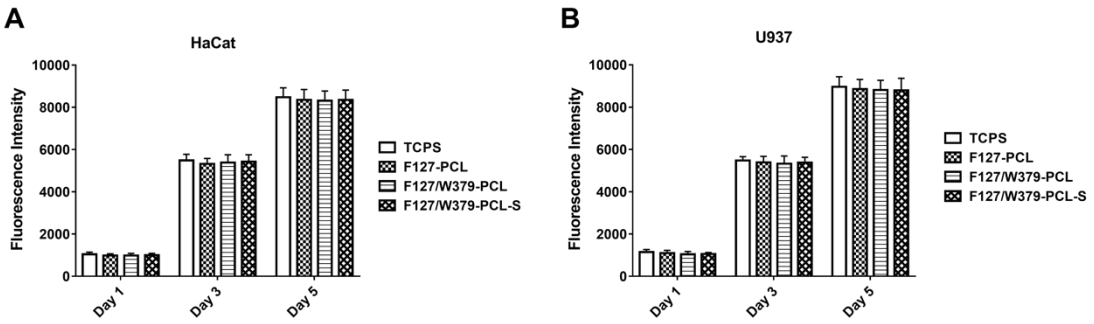

Figure S5. *In vitro* cytotoxicity test of W379 peptide-loaded PCL nanofiber membranes. (A) Alamar Blue cell viability test against HaCaT cells. (B) Alamar blue cell viability test against U937 cells. Each data point represents arithmetic mean ± SD values from four samples.

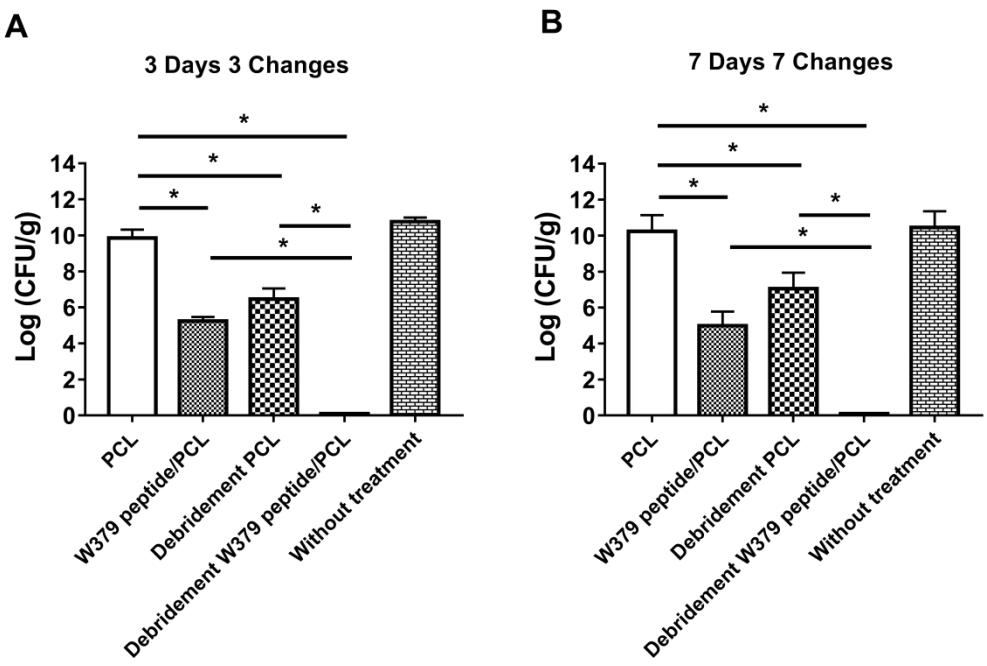

Figure S6. *In vivo* antibiofilm efficacy test of F127/W379-PCL-S nanofiber dressings. The MRSA and biofilm-containing chronic wounds created in type II diabetic mice were treated by F127/W379-PCL-S nanofiber dressings without and with debridement. PCL: Pluronic F127-PCL core-shell nanofiber membranes. W379 peptide/PCL: W379/pluronic F127-PCL core-shell nanofiber membranes. Debridement PCL: the wounds were conducted debridement and treated with pluronic F127-PCL core-shell nanofiber membranes. Debridement W379 peptide/PCL: the wounds were conducted debridement and treated with W379/pluronic F127-PCL core-shell nanofiber membranes. Without treatment: no treatment was applied to the wounds.

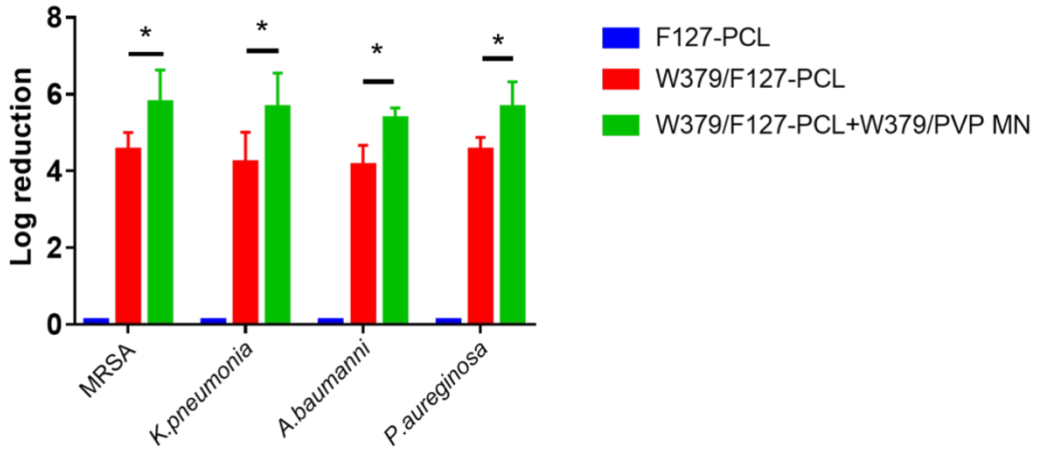

Figure 7. *In vitro* antibacterial activity. F127-PCL: Pluronic F127-PCL core-shell nanofiber membranes. W379/F127-PCL: W379/pluronic F127-PCL core-shell nanofiber membranes. W379/F127-PCL+W379/PVP MN: Janus-type antimicrobial dressing consisting of W379/pluronic F127-PCL core-shell nanofiber membranes and W379 loaded PVP microneedle arrays.

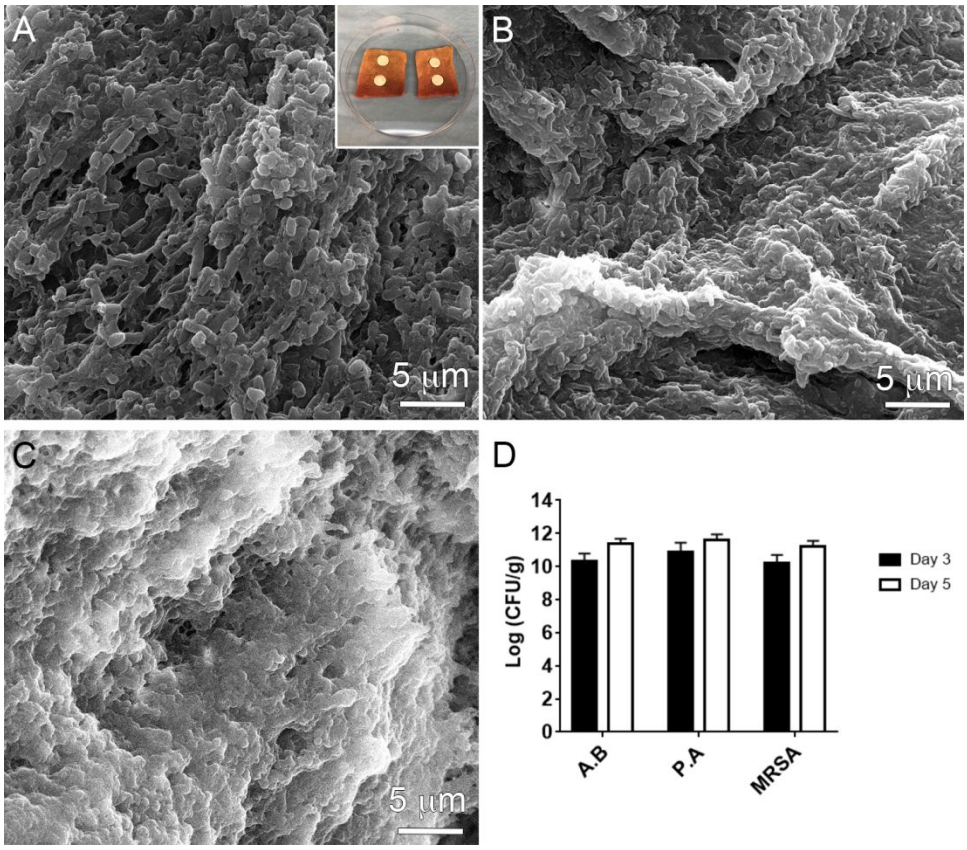

Figure S8. Biofilm formation on the excisional wounds created in human skin explants. (A-C) SEM images show the morphology of *A. baumanni*, *P. aeruginosa*, and MRSA biofilms on the excisional wounds in human skin explants. Inset: excisional wounds covered by Janus-type antimicrobial dressings (6 mm in diameter) in human skin explants. (B) Quantification of bacteria biofilms on excisional wounds in human skin explants.

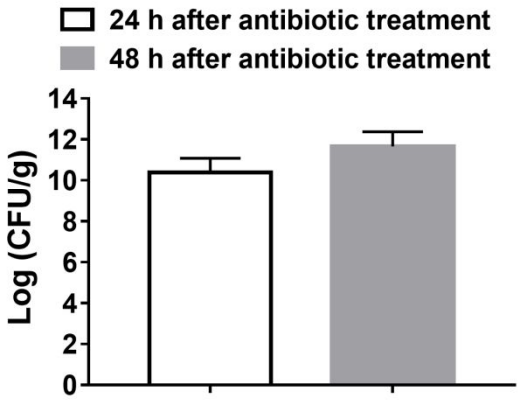

Figure S9. Quantification of bacterial load in the wound after 24 h and 48 h of MRSA inoculation and subsequent 24 h of 2% mupirocin treatment.

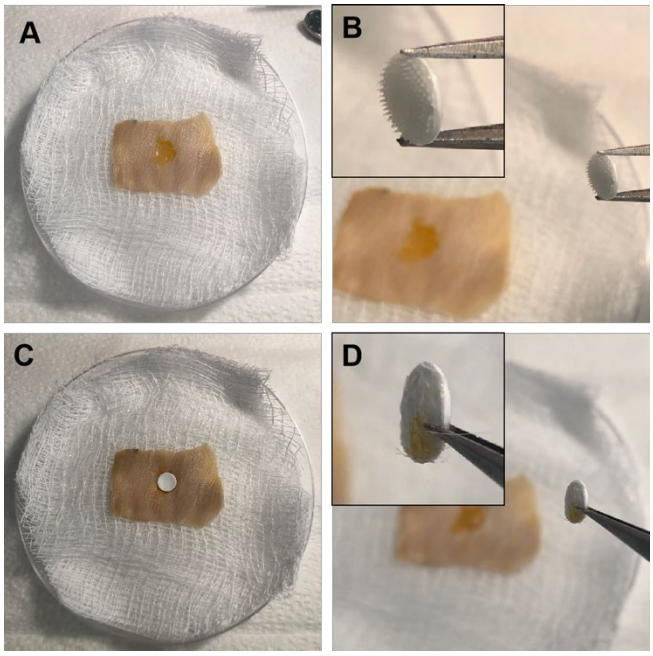

Figure S10. The dissolution of the microneedle arrays. (A) The biofilm was created on artificial wounds *ex vivo* before administration of dressings. (B) A Janus-type dressing consisting of a electrospun nanofiber membrane and an intact microneedle array. (C) The Janus-type dressing was administrated to the biofilm, and then the dressing was removed for observation with naked eyes. (D). After 3 min, the Janus-type dressing showed the electrospun nanofiber membrane alone, indicating the microneedle arrays were completely dissolved.

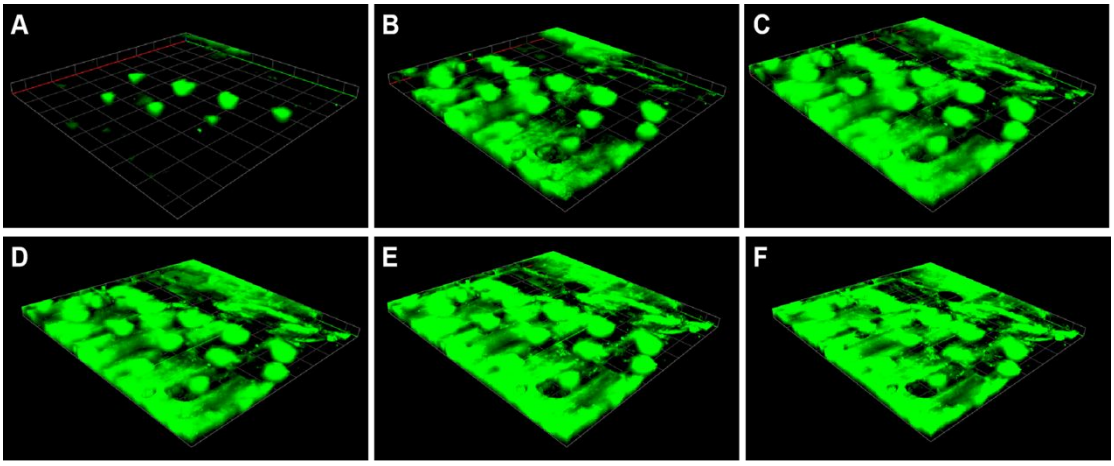

Figure S11. FITC-dextran diffusion and distribution in the biofilm created in human skin wounds *ex vivo* after administration of FITC-dextran containing microneedle arrays at different time points. (A) 0 min, (B) 20 min, (C) 40 min, (D) 60 min, (E) 80 min, (F) 100 min. The fluorescent region increased dramatically with increasing the administration time, revealing the FTIC-dextran can effectively diffuse to the surrounding area in biofilms.

Video S1. Animations of the peptide diffusion in the biofilm layer over time for the control. $D = 1 \times 10^{-12} m^2/s$.

Video S2. Animations of the peptide diffusion in the biofilm layer over time for the microneedle patch. $D = 1 \times 10^{-12} m^2/s$ and d = 150 μm.

Video S3. Animations of the peptide diffusion in the biofilm layer over time for the control. $D = 1 \times 10^{-12} m^2/s$.

Video S4. Animations of the peptide diffusion in the biofilm layer over time for the microneedle patch. $D = 1 \times 10^{-12} m^2/s$ and d = 300 μm.

Video S5. Animations of the peptide diffusion in the biofilm layer over time for the control. $D = 5 \times 10^{-13} m^2/s$.

Video S6. Animations of the peptide diffusion in the biofilm layer over time for the microneedle patch. $D = 5 \times 10^{-13} m^2/s$ and d = 150 μm.

Video S7. Animations of the peptide diffusion in the biofilm layer over time for the control. $D = 5 \times 10^{-13} m^2/s$.

Video S8. Animations of the peptide diffusion in the biofilm layer over time for the microneedle patch. $D = 5 \times 10^{-13} m^2/s$ and d = 300 μm.

Video S9. Animations of the peptide diffusion in the biofilm layer over time for the control. $D = 1 \times 10^{-13} m^2/s$.

Video S10. Animations of the peptide diffusion in the biofilm layer over time for the microneedle patch. $D = 1 \times 10^{-13} m^2/s$ and d = 150 μm.

Video S11. Animations of the peptide diffusion in the biofilm layer over time for the control. $D = 1 \times 10^{-13} m^2/s$.

Video S12. Animations of the peptide diffusion in the biofilm layer over time for the microneedle patch. $D = 1 \times 10^{-13} m^2/s$ and d = 300 μm.